Phylogenetic and ontogenetic changes of the anatomical organization and modularity in the skull of archosaurs

Short title: Evolution of network anatomy in archosaurian skulls

Hiu Wai Lee[1,2], Borja Esteve-Altava[3*], Arkhat Abzhanov[1,2*]

Affiliations:

[1] Imperial College London

[2] Natural History Museum, UK

[3] Institute of Evolutionary Biology (UPF-CSIC), Department of Experimental and Health Sciences, Pompeu Fabra University, Barcelona, Spain.

* Corresponding authors: borecal@gmail.com (B.E.A.), a.abzhanov@imperial.ac.uk (A.A.)

Abstract

Comparative anatomy studies of the skull of archosaurs provide insights on the mechanisms of evolution for the morphologically and functionally diverse species of crocodiles and birds. One of the key attributes of skull evolution is the anatomical changes associated with the physical arrangement of cranial bones. Here, we compare the changes in anatomical organization and modularity of the skull of extinct and extant archosaurs using an Anatomical Network Analysis approach. We show that the number of bones, their topological arrangement, and modular organization can discriminate between birds, non-avian dinosaurs, and crurotarsans, and between extant and extinct species. By comparing within the same framework juveniles and adults for crown birds and alligator (*Alligator mississippiensis*), we find that adult and juvenile alligator skulls are topologically similar, whereas juvenile bird skulls have a morphological complexity and anisomerism more similar to that of non-avian dinosaurs and crurotarsans than to their adult forms. Clade-specific ontogenetic differences in skull organization, such as extensive postnatal fusion of cranial bones in crown birds, can explain this pattern. The fact that juvenile and adult skulls in birds do share a similar anatomical integration suggests the presence of specific constraint in their ontogenetic growth.

Keywords: Comparative Anatomy; Cranium; Anatomical Network Analysis; Birds; Crocodiles; craniofacial evolution, Archosauria

INTRODUCTION

The skulls of archosaurs are morphologically and functionally diverse, with clade-specific specialized features that set apart crurotarsans (extant crocodilians and their stem lineage) from avemetatarsalians (birds and non-avian dinosaurs) (Gauthier, 1986; Benton & Clark, 1988; Sereno, 1991; Juul, 1994; Benton, 1999; 2004; Irmis et al. 2007; reviewed in Brusatte et al. 2010b). The evolution and diversification of the skull of archosaurs have been associated with changes in the patterns of phenotypic integration and modularity (Sadleir & Makovicky, 2008; Goswami et al. 2009; Hallgrímsson et al. 2009; Felice & Goswami, 2018; Felice et al. 2019; reviewed by Klingenberg, 2008). A differential integration among skull regions led to the organization of the skull around anatomical modules that can evolve, function, and develop semi-independently from one another. Bones within a same module tend to co-vary in shape and size more with each other than with bones from other such variational modules (Olson & Miller, 1958; Wagner & Altenberg, 1996; Eble, 2005; Wagner et al. 2007). In addition, the bones of the skull can also modify their physical articulations so that some groups of bones are more structurally integrated than others, and hence, we can recognize them as distinct anatomical-network modules (Esteve-Altava et al. 2011; Esteve-Altava, 2017). The relationship between anatomical-network modules and variational modules is not yet fully understood, but it is thought for network anatomy to constrain growth patterns and shape variation (Chernoff & Magwene, 1999; Esteve-Altava et al. 2013b; Rasskin-Gutman & Esteve-Altava, 2018).

There are three main hypotheses regarding the modularity of the skull of archosaurs. We proposed earlier in Sanger et al. (2011) the Tripartite Hypothesis, which divides the skull into three morpho-functional modules: the rostral, orbital, and braincase; we observed that patterns of variation from *Anolis* divide the skull into anterior and posterior modules. Piras and colleagues (2014) observed modules in crocodile skulls divide the skull into rostrum and postrostrum, based on biological functions, such as biting. Finally, Felice and colleagues (2019b) found that

landmarks that delineate the shape of archosaurian skulls are divided into variational modules based on their patterns of integration.

Changes in the anatomical organization of the skull in archosaurs have been concomitant with a broader evolutionary trend in tetrapods toward a reduction in the number of skull bones due to loses and fusions, a phenomenon known as the Williston's law (Gregory et al. 1935; Esteve-Altava et al. 2013a; 2014). Understanding how the bones are arranged relative to each other allows us to measure the anatomical complexity and organization of body parts, and explain how structural constraints might have influenced the direction of evolution (Esteve-Altava et al. 2013a; 2014; 2015; 2019). Recently, Werneburg and colleagues (2019) have compared the skull topology of a highly derived *Tyrannosaurus rex*, *Alligator mississipensis* and *Gallus gallus* with an opossum, a tuatara, and a turtle. However, the specific anatomical changes in the organization of the archosaur skull during their evolutionary transitions more generally have never been characterized. When applied to archosaurs, a network-based approach can highlight how skull topology changes in both evolutionary and developmental scales.

Here, we compared the anatomical organization and modularity of the skull of archosaurs using Anatomical Network Analysis (Rasskin-Gutman & Esteve-Altava, 2014). We created network models of the skull for 21 species of archosaurs, including taxa representing key evolutionary transitions from early pseudosuchians to crocodiles, from non-avian theropods to modern birds, and from paleognath birds to neognaths (Fig. 2). Our dataset also includes a representative ornithischian, a sauropodomorph, and a basal saurischian (Supplementary Information 1) for comparison. To understand the significance of the ontogenetic transitions in archosaur skulls, we provided our dataset with juvenile skulls for extant birds and alligator.

Network models of the skull were built by coding individual cranial bones and their articulations with other bones as the nodes and links of a network, respectively (Fig. 1). Network modules, defined as a group of bones with more articulations among them than to other bones outside the module, were identified heuristically using a community detection algorithm (see Methods for details). We compared skull architectures using topological variables (i.e. network parameters) that capture whole-skull anatomical feature (see Esteve-Altava et al. 2013a; Rasskin-Gutman & Esteve-Altava, 2014; Esteve-Altava, 2017, for details on the modelling and analysis of anatomical networks).

RESULTS

Topological discrimination of skull bones

A Principal Component Analysis (PCA) of the eight topological variables measured in skull network models discriminates skulls with different anatomical organizations (Figs. S1-S3). When all taxa are compared together, the first three principal components (PCs) explain 89.4% of the total variation of the sample. PC1 (57.5%) discriminates skulls by number of their bones (N), density of connections (D), and degree of modularity (P). PC2 (21.3%) discriminates skulls by their degree of integration (C) and anisomerism (H). Finally, PC3 (10.6%) discriminates skulls by whether bones with similar number of articulations connect with each other (A). PERMANOVA tests confirm that different skull anatomies map onto different regions of the morphospace. Thus, we can discriminate: Avialae (Aves plus *Ichthyornis dispar*, and *Archaeopteryx lithographica*) versus non-Avialae ($F_{1,23} = 4.885$, $p = 0.0036$; Fig. 3B); Neornithes plus toothless archosaurs versus archosaurs with teeth ($F_{1,23} = 8.507$, $p = 3 \times 10^{-4}$; Fig. 3C); Aves (include all modern birds) versus Crurotarsi versus non-avian Dinosauria ($F_{2,22} = 5.055$, $p = 2\times10^{-4}$; Fig. 3D); and extant and extinct species ($F_{1,23} = 6.169$, $p = 9.999\times10^{-5}$; Fig. S1C). However, we find no statistically

significant difference in morphospace occupation between crurotarsans and avemetatarsalians ($F_{1,23} = 1.374$, $p = 0.2428$, Figs. S1D).

When all avians are excluded from the comparison, the first three PCs explain 80.9% of the total variation (Figs. S4-6). PC1 (44.3%) discriminates skulls by the density of their inter-bone connections (D) and effective proximity (L). PC2 (21.7%) discriminates skulls by the number of bones and their articulations (N and K). Finally, PC3 (14.9%) discriminates skulls by their anisomerism (H) and whether bones with the same number of connections connect to each (A). PERMANOVA tests discriminate between Crurotarsi and non-avian Dinosauria ($F_{1,17} = 3.456$, $p = 0.0137$; Fig. S4C), and between extant and extinct species ($F_{1,17} = 4.299$, $p = 0.0033$; Fig. S4C).

When only adult birds are excluded, the first three PCs explain 84.6% of the topological variation (Figs. S7-9). PC1 (41.4%), PC2 (24.2%), and PC3 (15.5%) discriminate skull similarly as when all birds are excluded (see above). PERMANOVA tests discriminate between juvenile birds, crurotarsans, and non-avian dinosaurs ($F_{2,19} = 3.189$, $p = 0.0023$; Fig. S7D), and between extant and extinct species ($F_{1,20} = 4.282$, $p = 0.0032$; Fig. S7C).

Regardless of the subsample compared, we found no statistically significant difference in morphospace occupation between taxa stratified by flying ability and diet (Fig. S1E, see Supplementary Information 4 for details). This suggests that changes in cranial network-anatomy (i.e. how bones connect to each other) are independent of both dietary adaptations and the ability to fly.

Besides differences in morphospace occupation, we found no significant changes in the level of topological disparity among archosaur skulls during their over 250 million years of evolution at any key diversification events (Fig. 4).

Number of network modules

The number of network modules identified in archosaur skulls ranged from one (i.e. fully integrated skull) in adult birds *Nothura maculosa* (the spotted tinamou) and *Geospiza fortis* (medium ground finch) to eight in non-avian dinosaurs *Dilophosaurus wetherilli* and *Coelophysis bauri* (Table S12). The number of network modules within the studied taxa decreases during evolution of both major archosaurian clades: from 6 (*Riojasuchus tenuisceps*) to 5 (*Aetosaurus ferratus*, *Desmatosuchus haplocerus*, and *Sphenosuchus acutus*), and then to 4 (*Dibothrosuchus elaphros* to all crocodilians) modules in Crurotarsi; from 6 (*Citipati osmolskae* and *Velociraptor mongoliensis*) to 5 (*Archaeopteryx*), and then to 4 (*Ichthyornis* and juvenile modern birds) modules in theropod-juvenile bird transition (Fig. 5A and 5B, Table S12). Community detection algorithms found no modular division of the skull in adult *Nothura* and *Geospiza*. Most likely because these skulls are highly integrated due to the extensive cranial bone fusion in adults, which, in turn, results in a network with very few nodes. The only exception is the five modules in the adult *Gallus gallus* (chicken), which has one more than its juvenile form, despite its extensive fusion. In general, skull networks are clearly partitioned into modules, as shown by Q values ranging from 0.360 ± 0.089 to 0.568 ± 0.052: the modular partitions identified by the algorithm are better than expected at random.

Comparison of network modules with variational modules

We compared the partition of every skull into network modules with the variational modules reported in previous studies. We found that network modules for most archosaurs (21 out of 25 skulls) have the highest similarity to those reported by Felice et al. (2019): NMI ranging from 0.3 to 0.74 (Table S8, Supplementary Information 6). Exceptions are *Aetosaurus* (48.7%) and *Crocodylus moreletii* (74%) that are more similar to the modules from the Tripartite Hypothesis (Sanger et al. 2011); juvenile *Alligator* (56%) that is more similar to the modules based on *Anolis*

skulls (Sanger et al. 2011); and *Compsognathus longipes* (31.1%) that is more similar to modules from Piras et al. (2014

When compared with modules identified by Felice et al. (2019), some of the network modules reported here, such as the rostral and cranial modules (shown as blue and red modules in Fig. 5 and Table S4) appear to be composed of elements similar to those described as variational modules (more details in Supplementary Information 2). The supraoccipital and basioccipital bones were part of the same topology-defined (Supplementary Information 2, Table S4, Fig. 5) and shape-defined module in most taxa, perhaps due to its functional importance in connecting the vertebral column with the skull (Felice et al. 2019).

DISCUSSION

Occupation of morphospace and evolution of skull architecture

The two major groups of archosaurs (Crurotarsi and Avemetatarsalia) show an analogous trend towards a reduction in the number of skull bones (Table S10; Supplementary Information 3), in line with the Williston's Law, which states that vertebrate skulls tend to become more specialized with fewer bones as a result of fusions of neighboring bones during evolution (Sidor, 2001; McShea & Hordijk, 2013; Esteve-Altava et al. 2013a). This reduction in the number of bones and articulations, together with an increase in density, is also present in aetosaurs and sphenosuchians (Table S10). We also observed fusion of paired bones into new unpaired ones: for example, left and right frontals, parietals, and palatines are fused through their midline suture in the more derived taxa (Table S6). Bone fusion in extant species produced skulls that are more densely connected and are more modular than the skulls of extinct species (Fig. S1C). It was previously suggested that the more connected skulls would have more developmental and functional inter-

dependences among bones, and, hence, they would be more evolutionarily constrained (Esteve-Altava et al. 2013b; Rasskin-Gutman & Esteve-Altava, 2018). Similarly, avian cranium with strongly correlated traits have lower evolutionary rates and are less diverse (Felice & Goswami 2018).

Bhullar et al (2016) pointed out that avian kinesis relies on their loosely integrated skulls with less contact and, thus, skulls with highly overlapping bones would be akinetic. This contradicts our observations here that kinetic crown birds have more complex and integrated skulls than akinetic crurotarsans and partially kinetic *Riojasuchus* (Baczko & Desojo, 2016). The reason could be that Bhullar et al (2016) factored in how much connective tissue and space are available for specialized muscles to carry their functions, but not the total number of connections possible from the number of bones in these taxa. More recently, Werneburg and colleagues (2019) showed *Tyrannosaurus*, suspected to have kinesis, also has a higher density when compared to akinetic *Alligator* but lower density when compared to the more derived, kinetic *Gallus*.

Crurotarsi

The aetosaurs, *Aetosaurus* and *Desmatosuchus*, and the sphenosuchians, *Sphenosuchus* and *Dibothrosuchus*, show an increase in complexity within their lineages. The more derived aetosaur *Desmatosuchus* has a fused skull roof (parietal fused with supraoccipital, laterosphenoid, prootic and opisthotic) and toothless premaxilla that are absent in the less derived aetosaur *Aetosaurus* (Small, 1985; 2002; Schoch, 2007). In contrast, basal and derived sphenosuchian are more topologically similar. Their main difference is that basipterygoid and epiotic are separate in *Sphenosuchus* but are fused with other bones in the more derived *Dibothrosuchus* (Walker, 1990; Wu & Chatterjee, 1993). When we compared aetosaurs and sphenosuchians, we found that sphenosuchians have a skull roof intermediately fused between *Aetosaurus* and *Desmatosuchus*:

interparietal sutures in both sphenosuchians are fused while supraoccipital, laterosphenoid, opisthotic, and prootic remain separate.

To understand cranial topology in Thalattosuchia, a clade with adaptations specialized for marine life, we included *Dakosaurus andiniensis*. These adaptations comprise nasal salt glands (Fernández & Gasparini, 2007), hypocercal tail, paddle-like forelimbs, ziphodont dentition, fusion of the inter-premaxillary suture, a fused vomer, and a short and high snout (Gasparini et al. 2006; Pol & Gasparini, 2009). Despite these adaptations, *Dakosaurus* has a cranial complexity closer to extant crocodilians by similarly having inter-frontal and inter-parietal fusions (Gasparini et al. 2006; Pol & Gasparini, 2009). In addition to the fused frontals and parietals, both *Crocodylus* and *Alligator* have a fused palate and a fused pterygoid.

In turn, crurotarsans first fuse the skull roof and skull base, followed by the fusion of the face (more details on Table S6). Interestingly, this resonates with the pattern of sutural fusion in alligator ontogeny, which cranial (i.e. frontoparietal) has the highest degree of suture closure followed by skull base (i.e. basioccipital-exoccipital) and then the face (i.e. internasal) (Bailleul et al. 2016), suggesting that the same mechanism may control topological changes in both ontogeny and evolution.

Avemetatarsalia

Avemetatarsalian transition is marked with a faster bone growth in more derived taxa, indicated by higher degree of vascularization, growth marks, and vascular canal arrangement (reviewed in Bailleul et al. 2019), more pneumatized skulls (reviewed in Gold et al. 2013), and a crurotarsan-like increase in complexity. The basal ornithischian *Psittaosaurus* lujiatunensis and basal saurischian *Eoraptor lunensis* are relatively close to each other on the morphospace (Fig. 3), with the *Psittacosaurus* skull showing slightly more density because of fused palatines, a trait which is

also observed in extant crocodilians and birds, and its extra rostral bone as observed in other ceratopsians (Sereno et al. 2010).

The basal sauropodomorph *Plateosaurus engelhardti* has the lowest clustering coefficient (i.e. lower integration) of archosaurs, suggesting that skulls of sauropodmorphs are less integrated than those of saurischians (Rasskin-Gutman & Esteve-Altava, 2014), accompanied by poorly connected bones (as seen in the network in Fig. 5C). Poorly connected bones, for example epipterygoid (which only has one connection), and some connections, such as the ectopterygoid-jugal articulation, are later lost in neosauropods (Upchurch et al. 2004; Button et al. 2016).

For theropods, the ceratosaurian *Coelophysis* is more derived and has a slightly more complex and specialized skull than the ceratosaurian *Dilophosaurus* (Tykoski & Rowe, 2004). These two ceratosaurians are close to each other on the morphospace (Fig. 3), suggesting that ceratosaurians occupy a region characterized by high heterogeneity and lower complexity, when compared to other archosaurs. *Compsognathus* is close to *Eoraptor* and *Riojasuchus* on the morphospace, its facial bones are also unfused, and it has a similar composition for its facial modules. These observations suggest an ancestral facial topology (see Fig. 5B, Table S6 and S8 for more details) that accompanies the ancestral magnitude of shape change in compsognathids (Bhullar et al. 2012). *Compsognathus'* lacrimal articulates with the maxilla, a feature also found in *Eoraptor* but rare in other theropods (Ostrom, 1978; Sereno et al. 1993; Barsbold & Osmolska, 1999; Peyer, 2006). It possesses an independent postorbital that is absent from *Ichthyornis* to modern birds. It also has an independent prefrontal that is absent in most Oviraptorsauria and Paraves (Smith-Paredes et al. 2018), including *Citipati*, *Velociraptor*, and from *Ichthyornis* to modern birds. Despite these ancestral features, the back of the skull and the skull base of *Compsognathus* are fused, similarly to other Paravians and modern birds.

The oviraptorid *Citipati* has a skull topology that occupies a morphospace within non-avian theropods, despite its unique vertically-oriented premaxilla and short beak (Norell et al. 2011; Bhullar et al. 2012). *Citipati* has an independent epipterygoid that is also present in some non-avian theropods and ancestral archosaurs, such as *Plateosaurus erlenbergiensis*, but which is absent in extant archosaurs (de Beer, 1937; Gauthier et al. 1988; Norell et al. 2011; Clark et al. 2002). *Citipati* also has fused skull roof (with fused interparietals), skull base, and face, marked with fused internasal, intermaxillary, and the avian-like inter-premaxillary sutures.

Velociraptor, similar to other dromaeosaurids, has rostraolaterally facing eyes. Its prefrontal bone is either absent or fused with the lacrimal while it remains separate in other dromaeosaurids (Norell et al. 1994; Barsbold & Osmolska, 1999; Currie & Dong, 2001). We observed a loss of the prefrontals from *Citipati* to modern birds, but not in more ancestral archosaurs or crurotarsans. Bones forming the *Velociraptor* basicranium, such as basioccipital, and basisphenoid are fused with other members of the basicranium (listed in Table S6). Despite having a similar number of bones and articulations to *Citipati*, the cranial bones in *Velociraptor* are more integrated with each other and are more likely to connect to bones with a different number of articulations (i.e. more disparity). Similar to *Compsognathus* and other primitive non-avian dinosaurs, *Velociraptor* has an ancestral facial topology with separate premaxilla, maxilla, and nasal.

Archaeopteryx and _Ichthyornis_ as intermediates between non-avian theropods and birds

The skull of *Archaeopteryx* occupied a region of the morphospace closer to non-avian dinosaurs and crurotarsans than to juvenile birds (Fig. 3). The distance of *Archaeopteryx* from crown birds and its proximity in the morphospace to *Velociraptor* and *Citipati* along the PC1 axis (Fig. 3) may reflect the evolving relationship between cranial topology and endocranial volume. In fact, *Archaeopteryx* has an endocranial volume which is intermediate between the ancestral non-avian dinosaurs and crown birds (Larsson et al. 2000; Alsono et al. 2004) and it is within the

plesiomorphic range of other non-avian Paraves (Balanoff et al. 2013). This makes *Archaoepteryx* closer to dromaeosaurid *Velociraptor* than to oviraptor *Citipati*, for both its skull anatomy and its endocranial volume (Balanoff et al. 2013). Modifications related to the smaller endocranial volume in *Archaeopteryx* include the unfused bones in the braincase, the independent reappearance of a separate prefrontal after the loss in Paraves (Smith-Paredes et al. 2018), a separate left and right premaxilla as observed in crocodilian snouts and ancestral dinosaurs, and the presence of separate postorbitals, which might restrict the fitting for a larger brain (Bhullar et al. 2012).

Relative to *Archaeopteryx*, *Ichthyornis* is phylogenetically closer to modern birds and occupies a region of the morphospace near to the juvenile *Gallus* (Fig. 3), and to other non-avian theropods when adult birds are removed (Figs. S4-6). This is likely explained by the similar modular division (as observed in Figs. 5B and 5D; Table S4), presence of anatomical features characteristic of modern birds, such as the loss of the postorbital bones, the fusion of the left and right premaxilla to form the beak, a bicondylar quadrate that form a joint with the braincase, and the arrangement of the rostrum, jugal, and quadratojugal required for a functional cranial kinetic system (Jollie, 1957; Bock, 1964; Clarke, 2004; Bhullar et al. 2016; Field et al. 2018).

Paleognath and neognath

Juvenile birds have a skull roof with relatively less fused bones with the interfrontal, interparietal, and frontoparietal sutures open, and a more fused skull base. Postorbital is already fused in all juvenile birds (i.e. after hatching). In the juvenile paleognath *Nothura*, the internasal and intermaxilla sutures are also closed, while they are open in juvenile neognaths. Collectively, juvenile neognaths show a skull anatomy with a fused cranial base, relatively less fused roof, and unfused face that resembles the anatomy of ancestral non-avian theropods. Unlike in non-avian theropods, frontal, parietal, nasal, premaxilla, and maxilla eventually fuse with the rest of the

skull in adult birds. However, in the palatal region not all the sutures are completely closed: the caudal ends of the vomers remained unfused in adult *Nothura*, which is a characteristic common in Tinamidae (Silveria & Höfling, 2007). A similar pattern of suture closure has been described in another paleognath, the emu, in which the sutures of the base of the skull close first and then the cranial and facial sutures close while palatal sutures remain open (Bailleul et al. 2016). The only difference is in *Nothura*, in which closure of major cranial sutures (frontoparietal, interfrontal, and interparietal) happens after the facial sutures closure. In summary, when compared with neognaths, the skull of the paleognath *Nothura* is more homogeneous and complex in both juvenile and adult stages. As the skull grows, its bones fuse and both its complexity and heterogeneity increase.

Within the neognaths, the skull of *Geospiza fortis* is more complex and more homogenous than either juvenile or adult *Gallus gallus*. Bones in *Geospiza* skull are more likely to connect with bones with the same number of connections than *Gallus* in the juvenile stage, but this is reversed in adult stage. This is because more bones connect with bones that have different number of connections in *Geospiza* skull while *Gallus* skull becomes more irregular with age. These two trajectories illustrate how the connectivity of each bone diversifies and becomes more specialized within a skull as sutures fuse together, as predicted by the Williston's law.

Like crurotarsans, major transitions in Avemetatarsalia are associated with the fusion first of the skull base, then the skull roof, and, finally, with the face (more details on Table S6). This is more similar to the temporal pattern of sutural closure during ontogeny in the emu (skull base first, skull roof second, facial third) than to that observed in alligator (cranial first, skull base second, facial third) (Bailleul et al. 2016), suggesting the same mechanism for ontogeny may have been co-opted in Avemetatarsalia evolution.

Ontogenetic differences in topology between birds and crocodilians

Our comparisons on network anatomy found that juvenile birds occupy a region of the morphospace that is closer to the less derived archosaurs and crurotarsans than to that occupied by adult birds (Fig. S1B and 2E). Juvenile birds have a degree of anisomerism of skull bones, which is more similar to their non-avian theropod ancestors. Their skull anatomical complexity is closer to that in crurotarsans and non-avian dinosaurs, while the pattern of integration is closer to that of adult birds. These similarities in complexity and heterogeneity may be explained by the comparably higher number and symmetrical spatial arrangements of circumorbital ossification centres in early embryonic stages (Smith-Paredes et al. 2018). For example, both crown avians and *A. mississippiensis* have two ossification centres that fuse into one for lacrimals (Rieppel, 1993; Smith-Paredes et al. 2018). Meanwhile, ossification centres that form the prefrontal and postorbital, fuse in prenatal birds but remain separate in non-avian dinosaurs (Rieppel, 1993; Maxwell & Larsson, 2009; Smith-Paredes et al. 2018). These ossification centres later develop into different, but overlapping, number of bones and arrangement in juvenile birds (27 – 34 bones) and adult theropods (32 – 44 bones) with discrepancies explained by the heterochronic fusion of ossification centres (Table S10).

Following postnatal fusions and growth, bird skulls become more heterogeneous and their bones more connected and topologically closer to each other (Figs. 3C and 6; Table S10). This makes avian skull bones more diverse and functionally integrated. Simultaneously, skull topology in birds diversifies with ontogeny within their lineage, as shown by the ontogenetic trajectories of *Gallus*, *Nothura*, and *Geospiza* (Figs. 3C and 6). Skull topological disparity with (Fig. 4A) and without adult birds (Fig. 4B) suggests that such topological diversity within birds arose around 50 million years ago, when modern bird lineages diversified (Event D on Fig. 4, Brusatte et al. 2015; Jarvis et al. 2014). Thus, bones developed from ossification centres shared among crurotarsans

and avemetatarsalia, interact as modules with ancestral heterogeneity and complexity will later fuse and diversify to produce skulls of adult birds.

The skulls of birds, crocodilians, and dinosaurs develop from ossification centres with comparable spatial locations in the embryonic head (Smith-Paredes et al. 2018). When both phylogenetic and ontogenetic cranial shape variation was compared among crocodilians, Morris and colleagues (2019) showed that at mid- to late embryonic stages, cranial shapes originated from a conserved region of skull shape morphospace. They suggested that crocodilian skull morphogenesis at early and late embryonic stages are controlled by signaling molecules that are important in other amniotes as well, such as *Bmp4*, *calmodulin*, *Sonic hedgehog* (*Shh*); and *Indian hedgehog* (Abzhanov et al. 2004; Abzhanov et al. 2006; Hu & Marcucio, 2009a;b; Mallarino et al. 2011; Hu & Marcucio, 2012; Ahi, 2016; Morris et al. 2019). Then, from late prenatal stages onward, snout of crocodilians narrows (Watanabe & Slice, 2014) and elongates following different ontogenetic trajectories to give the full spectrum of crocodilian cranial diversity (Morris et al. 2019).

Another major transformation in archosaurian evolution is the origin of skulls of early and modern birds from the snouted theropods. This transition involved two significant heterochronic shifts (Bhullar et al. 2012; 2015). First, avians evolved highly paedomorphic skull shapes compared to their ancestors by developmental truncation (Bhullar et al. 2012). Then, a peramorphic shift where primitively paired premaxillary bones fused and the resulting beak bone elongated to occupy much of the new avian face (Bhullar et al. 2015). By comparison, the skull of *Alligator* undergoes extensive morphological change and closing of the interfrontal and interparietal sutures during embryogenesis followed by prolonged postnatal and maturation periods, with the lack of suture closure and even widening of some sutures (Padian et al. 2001; Bailleul et al. 2016). Bailleul and colleagues (2016) suggested mechanisms that inhibit suture

closure, rather than bone resorption, cause the alligator sutures to remain open during ontogeny. Nevertheless, juvenile and adult alligators share the same cranial topology featuring similar module compositions and both occupy a region of morphospace close to *Crocodylus* (Fig. 5D; Table S4 and S10). Such topological arrangement suggests that conserved molecular, cellular, and developmental genetic processes underlie skull composition and topology in crocodilians. Likewise, oviraptorid dinosaurs, as represented by *Citipati*, display their own unique skull shape and ontogenetic transformation (Bhullar et al. 2012), while retaining a topology conserved with other theropods. This suggests that developmental mechanisms are conserved among theropods.

The process of osteogenesis determines the shape and topology of the skull. In chicken embryo, inhibition of FGF and WNT signaling prevented fusion of the suture that separates the left and right premaxilla, disconnected the premaxilla-palatine articulation and changed their shapes giving the distal face a primitive snout-like appearance (Bhullar et al. 2015). The site of bone fusion in experimental unfused, snout-like chicken premaxilla showed reduced expression of skeletal markers *Runx2*, *Osteopontin*, and the osteogenic marker *Col I* (Bhullar et al. 2015), implying localized molecular mechanisms regulating suture closure and shape of individual cranial bones. Thus, changes in gene expression during craniofacial patterning in avians (Hu et al. 2003; Abzhanov et al. 2007; Brugmann et al. 2007; Hu & Marcucio, 2009a;b; 2012), non-avian dinosaurs, and crocodilians (Bhullar et al. 2015; Morris et al. 2019) underlie clade-specific differences in skull anatomical organization resulting from the similar patterns of bone fusion of bones.

Finally, we observe some network modules where bones within the same modules in juveniles will later fuse in adult birds, but not in *A. mississippiensis* (Supplementary Information 5; Fig. 5E, Table S4). For example, in *Nothura*, the bones grouped in the beak module in the juvenile (premaxilla, nasal, parasphenoid, pterygoid, vomer, and maxilla) will later fuse during formation

of the upper beak in the adult. In *A. mississippiensis*, premaxilla, maxilla, nasal, lacrimal, prefrontal, jugal, frontal, and ectopterygoid are also in the same juvenile snout module, but remain separate structures in adult. These findings suggest that bones within the same module are likely to fuse together in ontogeny but doing so is a lineage-specific feature.

Comparisons of juveniles and adults for extant birds and the alligator revealed ontogenetic changes linked to the evolution of the skull organization in archosaurs. Whereas the anatomical organization of the skull of juvenile alligators resembles that of adults, the anatomy of juvenile modern birds is closer to that of non-avian dinosaurs than to that of adult avians in terms of morphological complexity and anisomerism, probably due to the spatial arrangements of ossification centres at embryonic stages (Rieppel, 1993; Maxwell & Larsson, 2009; Smith-Paredes et al. 2018). More specifically, the differences in skull organization between crown birds and non-avian dinosaurs could be explained by postnatal fusion of bones.

CONCLUSION

A network-based comparison of the cranial skeletal anatomy of archosaurs shows that differences within and among archosaurian clades are associated with an increase of anatomical complexity, a reduction in number of bones (as predicted by the Williston's Law), and an increase of anisomerism marked by bone fusion, for both crurotarsans and avemetatarsalians. Our findings indicate that the anatomical organization of the skull is controlled by developmental mechanisms that diversified across and within each lineage: heterotopic changes in craniofacial patterning genes, heterochronic prenatal fusion of ossification centres (Rieppel, 1993; Maxwell & Larsson, 2009; Smith-Paredes et al. 2018), and lineage-specific postnatal fusion of sutures. Some of these mechanisms have been shown to be conserved in other tetrapods. For example, heterotopy of

craniofacial patterning genes also took place between chick and mice embryos (Brugmann et al. 2007; Hu & Marcucio, 2009a; b). Hu and Marcucio (2009b) showed that mouse frontonasal ectodermal zone could alter the development of the avian frontonasal process, suggesting a conserved mechanism for frontonasal development in vertebrates. Our findings illustrate how a comparative analysis of the anatomical organization of the skull can reveal common and disparate patterns and processes shaping skull evolution in vertebrates.

MATERIAL AND METHODS

We compared the anatomy of the skull of archosaurs focusing on the pattern of bone-bone articulation using an Anatomical Network Analysis (as detailed in Esteve-Altava et al. 2013a; Rasskin-Gutman and Esteve-Altava 2014; Esteve-Altava 2017).

Sampling

We sampled extinct and extant species, and for some forms also adults and juveniles to account for ontogenetic trends within archosaurs. Namely, adults *Aetosaurus ferratus, Archaeopteryx lithographica, Citipati osmolskae, Coelophysis bauri, Compsognathus longipes, Dakosaurus andiniensis, Desmatosuchus haplocerus, Dibothrosuchus elaphros, Dilophosaurus wetherilli, Eoraptor lunensis, Ichthyornis dispar, Plateosaurus engelhardti, Psittacosaurus lujiatunensis, Riojasuchus tenuisceps, Sphenosuchus acutus, Velociraptor mongoliensis, Gallus gallus, Geospiza fortis* and *Nothura maculosa*; and juveniles *Gallus gallus, Geospiza fortis, Nothura maculosa* and *Alligator mississippiensis*. Within our sample, eight species represent the transition from crurotarsan archosaur to crocodile and 13 species represent the transition from theropods to modern birds as described by Bhullar et al (2012), Brusatte et al. (2010a), Galton & Upchurch

(2004), Hailu & Dodson (2004), Holtz & Osmolska (2004), Nesbitt (2011), Norell & Makovicky (2004), Padian (2004), Tykoski & Rowe (2004), and Upchurch et al (2004).

Phylogenetic Context

We created a phylogenetic tree (Figure 2) following Bhullar et al (2012), Brusatte et al. (2010a), Galton & Upchurch (2004), Hailu & Dodson (2004), Holtz & Osmolska (2004), Nesbitt (2011), Norell & Makovicky (2004), Padian (2004), Tykoski & Rowe (2004), and Upchurch et al (2004). The tree was calibrated using the R package paleotree by the conservative "equal" method (Brusatte et al. 2008; Lloyd et al. 2012); branching events were constrained using the minimum dates for known internal nodes based on fossil data from Benton and Donoghue (2007) (Table S3) and the first and last occurrences of all 21 species from the Paleobiology Database using the paleobioDB package in R (Varela et al. 2019). Because there were two extinct *Nothura* species in the Paleobiology Database, the last occurrence for extant *Nothura* species was adjusted to 0 (Table S2).

Network Modelling

We built anatomical network models for each archosaur skull in our sample based on detailed literature descriptions and CT scans of complete skulls (see Supplementary Information 1). Skull bones were represented as the nodes of the network model and their pair-wise articulations (e.g. sutures and synchondroses) were represented as links between pairs of nodes (Figure 1). Skull network models were formalized as binary adjacency matrices, in which a 1 codes for two bones articulating and a 0 codes for absence of articulation. Bones that were fused together without trace of a suture in the specimens examined were formalized as a single individual bone.

Network Analysis

Following Esteve-Altava et al 2019, we quantified the following topological variables for each network model: the number of nodes (N), the number of links (K), the density of connections (D), the mean clustering coefficient (C), the mean path length (L), the heterogeneity of connections (H), the assortativity of connections (A), and the parcellation (P). The morphological interpretation of these topological variables has been detailed elsewhere (see Esteve-Altava et al. 2019; 2018). A summary is provided here. N and K represent the direct count of the number of individual bones and articulations observed in the skull. D is the number of connections divided by the maximum number of possible connections (it ranges from 0 to 1); D is a proxy measure for morphological complexity. C is the average number of neighboring bones that connect to one another in a network (i.e., actual triangles of nodes compared to the maximum possible): a value close to 1 shows all neighboring bones connect to each other while a value close to 0 shows neighboring bones do not connect to each other; C is a proxy measure for anatomical integration derived from co-dependency between bones. L measures average number of links separating two nodes (it ranges from 1 to N-1); L is a proxy measure of anatomical integration derived from the effective proximity between bones. H measures how heterogeneous connections are in a network: skulls composed of bones with a different number of articulations have higher H values. If all bones had the same number of connections (i.e., H = 0), it means that all bones were connected in the same way and the skull had a regular shape. A measures whether nodes with the same number of connections connect to each other (it ranges from -1 to 1); H and A are a proxy measure for anisomerism or diversification of bones. P measures the number of modules and the uniformity in the number of bones they group (it ranges from 0 to 1); P is a proxy for the degree of modularity in the skull. Calculating P requires a given partition of the network into modules (see next below).

Network parameters were quantified in R (R Core Team, 2018) using the igraph package (Csardi & Nepusz, 2006). Networks visualization was made using the visNetwork package (Almende et al. 2019).

Modularity Analysis

To find the optimal partition into network modules we used the algorithm infomap (Rosvall & Bergstrom, 2008), as implemented in the function cluster_infomap of igraph (Csardi & Nepusz, 2006). See Table S4 and Figure 5 for details. According to Newman and Girvan (2004) networks have a strong modularity if they have a Q value from 0.3 to 0.7, which shows that the output partition finds modules that are more integrated than expected at random.

We compared the partition of every skull into network modules with the variational modules reported in previous studies (Sanger et al. 2011; Piras et al. 2014; and Felice et al. 2019) using a normalized mutual information index (Danon et al. 2005). See Table S9 for details of the grouping of skull bones into variational hypotheses. This index provides a metric between 0 and 1 for the similarity or correspondence between a pair of grouping hypothesis.

Principal Component Analysis

We performed a Principal Component Analysis (PCA) of the eight topological variables with a singular value decomposition of the centered and scaled measures. On the resulting PCs, we used a PERMANOVA (10,000 iterations) to test whether topological variables discriminate between: (1) Avialae and non-Avialae; (2) adults and juveniles; (3) extinct and extant; (4) Crurotarsi and Avemetatarsalia; (5) Neornithes and non-Neornithes; (6) early flight, can do soaring flight, can do flapping flight, gliding, and flightless (details in Table S5); (7) Crurotasi, Dinosauria, and Aves; and (8) carnivorous, omnivorous, and herbivorous (dietary information in Supplementary Information 4). First, we performed the tests listed above for all archosaurs. Then we repeated these tests for a subsample that included all archosaurs except for all modern birds. Next, we repeated these tests for a subsample that included all archosaurs except for adult birds.

Disparity Through Time Analysis

We performed a disparity through time analysis to explore how topology diversity evolved. As variables, we used the PCs of a phylogenetic PCA with a Brownian model of evolution using the package phytools package (Revell, 2012) and the dtt function from geiger (Pennell et al. 2014) with 10,000 simulations for all taxa except the extant juveniles, first using all PCA (Fig. 4A) and then PC1 alone (Fig. S10A), and for all taxa except adult extant taxa using first all PCA (Fig. 4B) and then PC1 alone (Fig. S10B). We estimated the morphological disparity index (MDI) for the relative disparity compared to null hypothesis under Brownian motion.

ACKNOWLEDGEMENT

We thank Jake Horton for coding the adult and juvenile matrices for *Alligator mississippiensis* and *Crocodylus moreletii*, Patrick Campbell of Natural History Museum London for providing reptile specimens, Alfie Gleeson and Digimorph for CT scans of crocodiles, and staff from Natural History Museum library for literature search. BE-A has received financial support through the Postdoctoral Junior Leader Fellowship Programme from “la Caixa” Banking Foundation (LCF/BQ/LI18/11630002). HWL received Masters project funding from Imperial College London and Natural History Museum, London.

AUTHOR CONTRIBUTION

HWL, BE-A, AA designed the study.

HWL coded network models.

HWL and BE-A wrote the R scripts and performed the analyses.

All authors discussed the results and wrote the manuscript.

REFERENCES

Abzhanov A, Cordero D R, Sen J, Tabin CJ, Helms JA (2007). Cross-regulatory interactions between *Fgf8* and *Shh* in the avian frontonasal prominence. *Congenital Anomalies*, *47*(4), 136–148. https://doi.org/10.1111/j.1741-4520.2007.00162.x

Abzhanov A, Kuo WP, Hartmann C, Grant BR, Grant PR, Tabin CJ (2006). The calmodulin pathway and evolution of elongated beak morphology in Darwin's finches. *Nature*, *442*(7102), 563–567. https://doi.org/10.1038/nature04843

Ahi, EP (2016). Signalling pathways in trophic skeletal development and morphogenesis: Insights from studies on teleost fish. *Developmental Biology*, *420*(1), 11–31. https://doi.org/10.1016/j.ydbio.2016.10.003

Almende BV, Thieurmel B, Robert T (2019). visNetwork: Network Visualization using 'vis.js' Library. R package version 2.0.8. https://CRAN.R-project.org/package=visNetwork

Alonso PD, Milner AC, Ketcham RA, Cookson MJ, Rowe TB (2004). The avian nature of the brain and inner ear of *Archaeopteryx*. *Nature*, 430(7000), 666-669. doi: 10.1038/nature02706

Arthur W (2004). *Biased Embryos and Evolution*. Cambridge: Cambridge Univ. Press.

Baczko MB, Desojo JB (2016). Cranial anatomy and palaeoneurology of the archosaur *Riojasuchus tenuisceps* from the Los Colorados Formation, La Rioja, Argentina. *PLoS ONE* 11(2). https://doi.org/10.1371/journal.pone.0148575.

Bailleul AM, Scannella JB, Horner JR, Evans DC (2016). Fusion patterns in the skulls of modern archosaurs reveal that sutures are ambiguous maturity indicators for the Dinosauria. *PLoS ONE*, *11*(2), 1–26. https://doi.org/10.1371/journal.pone.0147687

Balanoff AM, Bever GS, Rowe TB, Norell MA (2013). Evolutionary origins of the avian brain. *Nature*, *501*(7465), 93–96. https://doi.org/10.1038/nature12424

Barsbold R, Osmolska H (1999). The skull of *Velociraptor* (Theropoda) from the Late Cretaceous of Mongolia. *Acta Palaeontologica Polonica* 442: 189–219. https://doi.org/10.1016/S0140-6736(95)90336-4.

Bastir M, Rosas A (2005). Hierarchical nature of morphological integration and modularity in the human posterior face. *Am. J Phys. Anthropol*, *128*, 26–34.

Benton MJ (1999). *Scleromochlus taylori* and the origin of dinosaurs and pterosaurs. *Philosophical Transactions of the Royal Society of London, Series B* 354, 1423–1446

Benton MJ (2004). Origin and Relationships of Dinosauria. *The Dinosauria*, edited by Weishampel DB, Dodson P, Osmólska H, 2nd ed., 7–19. University of California Press. https://doi.org/10.1525/california/9780520242098.003.0005.

Benton MJ, Clark JM (1988). Archosaur phylogeny and the relationships of the Crocodylia. In: Benton MJ (Ed.), *The Phylogeny and Classification of the Tetrapods: Systematics Association Special*, Volume 35A, pp. 295–338

Bhullar BAS, Hanson M, Fabbri M, Pritchard A, Bever GS, Hoffman S (2016). How to make a bird skull: major transitions in the evolution of the avian cranium, paedomorphosis, and the beak as a surrogate hand. *Integrative and Comparative Biology* 56 (3): 389–403. https://doi.org/10.1093/icb/icw069

Bhullar BAS, Marugán-Lobón J, Racimo F, Bever GS, Rowe TB, Norell MA, et al.(2012). Birds Have Paedomorphic Dinosaur Skulls. *Nature* 487 (7406): 223–26. https://doi.org/10.1038/nature11146.

Bhullar BAS, Morris ZS, Sefton EM, Tok A, Tokita M, Namkoong B, et al. (2015). A molecular mechanism for the origin of a key evolutionary innovation, the bird beak

and palate, revealed by an integrative approach to major transitions in vertebrate history. *Evolution*, *69*(7), 1665–1677. https://doi.org/10.1111/evo.12684

Bock WJ (1964). Kinetics of the avian skull. *Journal of Morphology* 114 (1): 1–41). https://doi.org/10.1002/jmor.1051140102.

Bock WJ (1999). Cranial kinesis revisited. *Zoologischer Anzeiger* 238 (1–2): 27–39.

Bookstein FL, Gunz P, Mitteroecker P, Prossinger H, Schaefer K, Seidler H (2003). Cranial integration in *Homo*: singular warps analysis of the midsagittal plane in ontogeny and evolution. *Journal of Human Evolution*, 167–187. https://doi.org/10.1016/S0047-2484(02)00201-4

Bright JA, Marugán-Lobón J, Cobb SN, Rayfield EJ (2016). The Shapes of Bird Beaks are Highly Controlled by Nondietary Factors. *Proceedings of the National Academy of Sciences of the United States of America* 113 (19): 5352–57. https://doi.org/10.1073/pnas.1602683113.

Brugmann SA, Goodnough LH, Gregorieff A, Leuch, P, ten Berge D, Fuerer C, et al (2007). Wnt signaling mediates regional specification in the vertebrate face. *Development*, *134*(18), 3283–3295. https://doi.org/10.1242/dev.005132

Brusatte SL, Benton MJ, Desojo JB, Langer MC (2010a). The Higher-Level Phylogeny of Archosauria (Tetrapoda: Diapsida). *Journal of Systematic Palaeontology* 8 (1): 3–47. https://doi.org/10.1080/14772010903537732.

Brusatte SL, Nesbitt SJ, Irmis RB, Butler RJ, Benton MJ, Norell MA (2010b). The origin and early radiation of dinosaurs. *Earth-Science Reviews*, *101*(1–2), 68–100. https://doi.org/10.1016/j.earscirev.2010.04.001

Chernoff B, Magwene PM (1999). Afterword. In: *Morphological Integration: Forty years later.* pp 319-353. University of Chicago Press, Chicago.

Cheverud JM (1984). Quantitative genetics and developmental constraints on evolution by

selection. *J Theor. Biol.* 110:155–71

Chikilian M, de Speroni NB (1996). Comparative Study of the Digestive System of Three Species of Tinamou. I. *Crypturellus tataupa*, *Nothoprocta cinerascens*, and *Nothura maculosa* (Aves: Tinamidae). *Journal of Morphology* 228: 77–88.

Clarke JA (2004). Morphology, phylogenetic taxonomy, and systematics of *Ichthyornis* and *Apatornis* (Avialae: Ornithurae). *Bull. Am. Mus. Nat. Hist.* 286, 1–179.

Csardi G, Nepusz T (2006). The Igraph Software Package for Complex Network Research, InterJournal, Complex Systems 1695. http://igraph.org.

Currie PJ, Dong Z (2001). New information on Cretaceous troodontids (Dinosauria, Theropoda) from the People's Republic of China. *Can. J Earth Sci.* 38, 1753–1766

Dumont M, Tafforeau P, Bertin T, et al. (2016). Synchrotron Imaging of Dentition Provides Insights into the Biology of *Hesperornis* and *Ichthyornis*, the 'Last' Toothed Birds. *BMC Evolutionary Biology* 16 (1): 1–28. https://doi.org/10.1186/s12862-016-0753-6.

Eble GJ (2005). Morphological modularity and macroevolution: conceptual and empirical aspects. In: Callebaut W, Rasskin-Gutman D, editors. *Modularity. Understanding the development and evolution of natural complex systems.* Cambridge, MA: MIT Press. 221–238.

Erdmann K (1940). Zur entwicklungsgeschichte der knochen im schädel des huhnes bis zum zeitpunkt des ausschlüpfens aus dem ei. *Zoomorphology*, *36*, 315–400.

Esteve-Altava B (2017). Challenges in identifying and interpreting organizational modules in morphology. *Journal of Morphology* 278 (7): 960–74. https://doi.org/10.1002/jmor.20690.

Esteve-Altava B, Marugán-Lobón J, Botella H, Rasskin-Gutman D (2011). Network models in anatomical systems. *Journal of Anthropological Sciences* 89 (1945): 175–84. https://doi.org/10.4436/jass.89016.

Esteve-Altava B, Marugán-Lobón J, Botella, H, Rasskin-Gutman, D (2013a). Structural constraints in the evolution of the tetrapod skull complexity: Williston's Law revisited using network models. *Evolutionary Biology* 40 (2): 209–19. https://doi.org/10.1007/s11692-012-

9200-9.

Esteve-Altava B, Marugán-Lobón J, Botella, H, Bastir M, Rasskin-Gutman, D (2013b). Grist for Riedl's mill: A network model perspective on the integration and modularity of the human skull. *Journal of Experimental Zoology Part B: Molecular and Developmental Evolution*, *320*(8), 489–500. https://doi.org/10.1002/jez.b.22524

Esteve-Altava B, Pierce SE, Molnar JL, Johnston P, Diogo R, Hutchinson JR (2019). Evolutionary Parallelisms of Pectoral and Pelvic Network-Anatomy from Fins to Limbs. *Science Advances* 5(5). https://doi.org/10.1126/sciadv.aau7459.

Felice RN, Goswami A (2018). Developmental Origins of Mosaic Evolution in the Avian Cranium. *Proceedings of the National Academy of Sciences of the United States of America* 115 (3): 555–60. https://doi.org/10.1073/pnas.1716437115.

Felice RN, Watanabe A, Cuff AR, et al. (2019). Evolutionary Integration and Modularity in the Archosaur Cranium. *Integrative and Comparative Biology*. https://doi.org/10.1093/icb/icz052.

Fernandez Blanco MV, Cassini GH, Bona P (2018). Skull ontogeny of extant caimans: a three-dimensional geometric morphometric approach. *Zoology*, *129*(November 2017), 69–81. https://doi.org/10.1016/j.zool.2018.06.003

Fernández M, Gasparini Z (2008). Salt glands in the Jurassic metriorhynchid *Geosaurus*: implications for the evolution of osmoregulation in Mesozoic marine crocodyliforms. *Naturwissenschaften* **95,** 79–84. https://doi.org/10.1007/s00114-007-0296-1

Field D J, Hanson M, Burnham D, et al. (2018). Complete Ichthyornis Skull Illuminates Mosaic Assembly of the Avian Head. *Nature* 557 (7703): 96–100. https://doi.org/10.1038/s41586-018-0053-y.

Foth C, Rauhut OWM (2013). Macroevolutionary and morphofunctional patterns in theropod skulls: A morphometric approach. *Acta Palaeontologica Polonica*, *58*(1), 1–16. https://doi.org/10.4202/app.2011.0145

Galton PM, Upchurch P (2004). Prosauropoda. *The Dinosauria*, edited by Weishampel DB, Dodson P, Osmólska H, 2nd ed., 232–58. University of California Press. https://doi.org/10.1525/california/9780520242098.003.0005.

Gauthier JA (1986). Saurischian monophyly and the origin of birds. *Memoirs of the California Academy of Sciences* 8, 1–55.

Gauthier JA, de Queiroz K (2001). Feathered Dinosaurs, Flying Dinosaurs, Crown Dinosaurs, and the Name "Aves." *New Perspectives on the Origin and Early Evolution of Birds: Proceedings of the International Symposium in Honor of John H Ostrom*, edited by J Gauthier and L.FGall, 7-41. New Haven: Peabody Mus. Nat. Hist., Yale Univ. http://si-pddr.si.edu/dspace/bitstream/10088/4690/3/2001Gau_deQOst.pdf.

Genbrugg A, Herrel A, Boone M, et al. (2011a). The head of the finch: The anatomy of the feeding system in two species of finches (*Geospiza fortis* and *Padda oryzivora*). *Journal of Anatomy* 219 (6): 676–95. https://doi.org/10.1111/j.1469-7580.2011.01437.x.

Genbrugge A, Heyde AS, Adriaens D, et al. (2011b). Ontogeny of the cranial skeleton in a Darwin's Finch (*Geospiza fortis*). *Journal of Anatomy* 219 (2): 115–31. https://doi.org/10.1111/j.1469-7580.2011.01388.x.

Goswami A, Smaers B, Soligo C, Polly PD (2014). The Macroevolutionary Consequences of Phenotypic Integration: From Development to Deep Time. *Philosophical Transactions of the Royal Society B: Biological Sciences* 369 (1649). https://doi.org/10.1098/rstb.2013.0254.

Gregory WK, Roigneau M, Burr ER, et al. (1935). Williston's law relating to the evolution of skull bones in the vertebrates. *American Journal of Physical Anthropology*, 20, 123–152. https://doi.org/10.1002/ajpa.1330200202.

Hall, B. K. (2005). Bones and cartila

Hailu Y, Dodson P (2004). Basal Ceratopsia. *The Dinosauria*, edited by Weishampel DB, Dodson P, Osmólska H, 2nd ed., 325–34. University of California Press. https://doi.org/10.1525/california/9780520242098.003.0005.

Hallgrímsson B, Jamniczky H, Young NM, et al. (2009). Deciphering the palimpsest: Studying the relationship between morphological Integration and phenotypic covariation. *Evol Biol* 36 (4): 355–76. https://doi.org/10.1007/s11692-009-9076-5.

Hallgrímsson B, Lieberman DE, Liu W, Ford-Hutchinson AF, Jirik FR (2007). Epigenetic interactions and the structure of phenotypic variation in the cranium. *Evolution, Development*, *9*(1), 76–91. https://doi.org/10.1111/j.1525-142X.2006.00139.x

Hansen TF, Houle D (2008). Measuring and comparing evolvability and constraint in multivariate characters. *Journal of Evolutionary Biology* 21: 1201–19. https://doi.org/10.1111/j.1420-9101.2008.01573.x.

Holtz TR Jr, Osmólska H (2004). Saurischia. The *Dinosauria*, edited by Weishampel DB, Dodson P, Osmólska H, 2nd ed., 21–24. University of California Press. https://doi.org/10.1525/california/9780520242098.003.0005.

Horton J (2018). An Anatomical Network Analysis of Crocodilian Skull Ecomorphology and Modularity. MSc Thesis. Imperial College London, London.

Horvath S, Dong J (2008). Geometric Interpretation of Gene Coexpression Network Analysis. *PLOS Computational Biology* 4 (8): e1000117. https://doi.org/10.1371/journal.pcbi.1000117.

Hu D, Marcucio RS (2009a). A SHH-responsive signaling center in the forebrain regulates craniofacial morphogenesis via the facial ectoderm. *Development*, *136*(1), 107–116. https://doi.org/10.1242/dev.026583

Hu D, Marcucio RS (2009b). Unique organization of the frontonasal ectodermal zone in birds and mammals. *Developmental Biology*, *325*(1), 200–210. https://doi.org/10.1016/j.ydbio.2008.10.026

Hu D, Marcucio RS (2012). Neural crest cells pattern the surface cephalic ectoderm during FEZ formation. *Developmental Dynamics*, *241*(4), 732–740. https://doi.org/10.1002/dvdy.23764

Hu D, Marcucio RS, Helms JA (2003). A zone of frontonasal ectoderm regulates patterning and growth in the face. *Development*, *130*(9), 1749–1758. https://doi.org/10.1242/dev.00397

Irmis RB, Parker WG, Nesbitt SJ, Liu J (2007). Early ornithischian dinosaurs: the Triassic record. *Historical Biology* 19, 3–22.

Jollie MT (1957). The head skeleton of the chicken and remarks on the anatomy of this region in other birds. *J Morphol*. 100, 389–436.

Juul L (1994). The phylogeny of basal archosaurs. *Palaeontologia Africana* 31, 1–38.

Klein N, Sander PM (2007). Bone histology and growth of the prosauropod dinosaur *Plateosaurus Engelhardti* von Meyer, 1837 from the Norian bonebeds of Trossingen (Germany) and Frick (Switzerland). *Special Papers in Palaeontology*, (77), 169–206.

Klingenberg CP (2008). Morphological Integration and Developmental Modularity. *Annual Review of Ecology, Evolution, and Systematics* 39 (1): 115–32. https://doi.org/10.1146/annurev.ecolsys.37.091305.110054.

Klingenberg CP (2014). Studying Morphological Integration and Modularity at Multiple Levels: Concepts and Analysis. *Philosophical Transactions of the Royal Society of London. Series B, Biological Sciences* 369 (1649): 20130249. https://doi.org/10.1098/rstb.2013.0249.

Klingenberg CP, Badyaev AV, Sowry SM, Beckwith NJ (2001). Inferring developmental modularity from morphological integration: analysis of individual variation and asymmetry in bumblebee wings. *Am. Nat*. 157:11–23

Klingenberg, CP, Leamy LJ (2001). Quantitative genetics of geometric shape in the mouse mandible. *Evolution* 55:2342–52.

Klingenberg CP, Marugán-Lobón J (2013). Evolutionary Covariation in Geometric Morphometric Data: Analyzing Integration, Modularity, and Allometry in a Phylogenetic Context. *Systematic Biology* 62 (4): 591–610. https://doi.org/10.1093/sysbio/syt025.

Klingenberg CP, Mebus K, Auffray JC (2003). Developmental integration in a complex morphological structure: how distinct are the modules in the mouse mandible? *Evol. Dev.*

5:522–31

Klingenberg CP, Zaklan SD (2000). Morphological integration between developmental compartments in the Drosophila wing. *Evolution* 54:1273–85

Larsson HCE, Sereno PC, Wilson JA (2000). Forebrain Enlargemant among Nonavian Theropod Dinosaurs. *Journal of Vertebrate Paleontology*, *20*(3), 615–618. Retrieved from https://doi.org/10.1671/0272-4634(2000)020[0615:FEANTD]2.0.CO;2

Marcot JD, Mcshea DW (2007). Increasing Hierarchical Complexity throughout the History of Life : Phylogenetic Tests of Trend Mechanisms. *Paleobiology* 33 (2): 182–200.

Martonoş C, Dumitru I, Dezdrobitu C, Blendea A, Damian A (2014). Anatomical Studies Concerning the Skeleton of the Head in the Alligator (*Alligator mississippiensis*). *Bulletin of University of Agricultural Sciences and Veterinary Medicine Cluj-Napoca - Veterinary Medicine* 71 (1): 152–59. https://doi.org/10.15835/buasvmcn-vm:71:1:9604.

Marugán-Lobón J, Buscalioni AD (2003). Disparity and Geometry of the Skull in Archosauria (Reptilia: Diapsida). *Biological Journal of the Linnean Society* 80 (1): 67–88. https://doi.org/10.1046/j.1095-8312.2003.00219.x.

Maxwell EE, Larsson HCE (2009). Comparative ossification sequence and skeletal development of the postcranium of palaeognathous birds (Aves: Palaeognathae). *Zool. J Linn. Soc.* 157, 169–196.

McShea DW, Hordijk W (2013). Complexity by Subtraction. *Evol Biol* 40(4): 504-520. https://doi.org/10.1007/s11692-013-9227-6

Morris ZS, Vliet KA, Abzhanov A, Pierce SE (2019). Heterochronic shifts and conserved embryonic shape underlie crocodylian craniofacial disparity and convergence. *Proceedings of the Royal Society Biological Sciences*, *286*, 20182389. https://doi.org/10.1098/rspb.2018.2389

Nesbitt SJ (2011). The Early Evolution of Archosaurs: Relationships and the Origin of Major Clades. *Bulletin of the American Museum of Natural History* 352 (352): 1–292.

https://doi.org/10.1206/352.1.

Newman MEJ, Girvan M (2004). Finding and evaluating community structure in networks. *Physical Review E - Statistical, Nonlinear, and Soft Matter Physics* 69 (22): 1–15. https://doi.org/10.1103/PhysRevE.69.026113.

Norell MA, Makovicky PJ, Bever GS, Balanoff AM, Clark JM, Barsbold R, Rowe T (2014). A Review of the Mongolian Cretaceous Dinosaur Saurornithoides (Troodontidae: Theropoda). *American Museum Novitates* 3654 (3654): 1–63. https://doi.org/10.1206/648.1.

Northcutt RG (2011). Evolving Large and Complex Brains. *Science* 332 (6032): 926–27. https://doi.org/10.1126/science.1206915.

Olsen AM, Westneat MW (2016). Linkage Mechanisms in the Vertebrate Skull: Structure and Function of Three-Dimensional, Parallel Transmission Systems. *Journal of Morphology* 277 (12): 1570–83. https://doi.org/10.1002/jmor.20596.

Ostrom JH (1978). The osteology of *Compsognathus longipes*. Zitteliana. 4: 73–118

Padian K (2004). Basal Avialae. The *Dinosauria*, edited by Weishampel DB, Dodson P, Osmólska H, 2nd ed., 210–31. University of California Press. https://doi.org/10.1525/california/9780520242098.003.0005.

Padian K, de Ricqle AJ, Horner JR (2001). Dinosaurian growth rates and bird origins. *Nature*, *412*, 405–408.

Padian K, Horner JR, de Ricqlès A (2004). Growth in small dinosaurs and pterosaurs: The evolution of archosaurian growth strategies. Journal of Vertebrate Paleontology, 24(3), 555–571. https://doi.org/10.1671/0272-4634(2004)024[0555:GISDAP]2.0.CO;2

Peyer K (2006). A Reconsideration of *Compsognathus* from the Upper Tithonian of Canjuers, Southeastern France. *Journal of Vertebrate Paleontology* 26 (January): 879–96. https://doi.org/10.1671/0272-4634(2006)26[879:AROCFT]2.0.CO;2.

Piras P, Buscalioni AD, Teresi L, Raia P, Sansalone G, Kotsakis T, Cubo J (2014). Morphological integration and functional modularity in the crocodilian skull. *Integrative Zoology*, *9*(4), 498–516. https://doi.org/10.1111/1749-4877.12062

R Core Team. (2018). R: A Language and Environment for Statistical Computing. R Foundation for Statistical Computing. Vienna, Austria. https://www.r-project.org/.

Rasskin-Gutman D, Esteve-Altava B (2014). Connecting the dots: anatomical network analysis in morphological evodevo. *Biological Theory* 9 (2): 178–93. https://doi.org/10.1007/s13752-014-0175-x.

Rasskin-Gutman D, Esteve-Altava B (2018). Concept of Burden in Evo-Devo. In Nuño de la Rosa L, Müller G (eds.), *Evolutionary Developmental Biology* (pp. 1–11). Springer, Cham. https://doi.org/10.1007/978-3-319-33038-9_48-1

Rieppel O (1993). Studies on skeleton formation in reptiles. v. Patterns of ossification in the skeleton of Alligator mississippiensis Daudin (Reptilia, Crocodylia). *Zool. J Linn. Soc.* 109, 301–325.

Rinehart LF, Lucas SG, Heckert AB, Spielmann JA, Celeskey MD (2009). The Paleobiology of *Coelophysis bauri* (Cope) from the Upper Triassic (Apachean) Whitaker Quarry, New Mexico, with Detailed Analysis of a Single Quarry Block. *New Mexico Museum of Natural History, Science*, no. Bulletin 45.

Rosvall M, Bergstrom CT (2008). Maps of Information Flow Reveal Community Structure in Complex Networks. *PNAS* 105 (1118). https://doi.org/10.1073/pnas.0706851105.

Sadleir RW, Makovicky PJ (2008). Cranial shape and correlated characters in crocodile evolution. J Evol. Biol. 21, 1578–1596. https://doi.org/0.1111/j.1420-9101. 2008.01602.x

Sander PM, Klein N (2005). Paleontology: Developmental plasticity in the life history of a prosauropod dinosaur. *Science*, *310*(5755), 1800–1802. https://doi.org/10.1126/science.1120125

Sanger TJ, Mahler DL, Abzhanov A, Losos JB (2012). Roles for modularity and constraint in the evolution of cranial diversity among anolis lizards. *Evolution*, *66*(5), 1525–1542. https://doi.org/10.1111/j.1558-5646.2011.01519.x

Schluter D (1996). Adaptive radiation along genetic lines of least resistance. *Evolution* 50:1766–74

Sereno PC (1991). Basal archosaurs: phylogenetic relationships and functional implications. *Society of Vertebrate Paleontology Memoir* 2, 1–53.

Sidor CA (2001). Simplification as a trend in synapsid cranial evolution. *Evolution* 55(7): 1419-1442

Smith-Paredes D, Núñez-León D, Soto-Acuña S, O'Connor J, Botelho J F, Vargas AO (2018). Dinosaur Ossification Centres in Embryonic Birds Uncover Developmental Evolution of the Skull. *Nature Ecology and Evolution* 2 (12): 1966–73. https://doi.org/10.1038/s41559-018-0713-1.

Tkach JS (1996). Multi-element osteohistological analysis of *Dilphosaurus wetherilli*. Abstracts of Papers, Fifty-sixth Annual Meeting, Society of Vertebrate Paleontology, American Museum of Natural History, New York, New York, October 16–19". Journal of Vertebrate Paleontology. 16 (3): 1A–80A. JSTOR 4523755

Tykoski RS, Rowe T (2004). Ceratosauria. The *Dinosauria*, edited by Weishampel DB, Dodson P, Osmólska H, 2nd ed., 47–70. University of California Press. https://doi.org/10.1525/california/9780520242098.003.0005.

Upchurch P, Barrett PM, Dodson P (2004). Sauropoda. The *Dinosauria*, edited by Weishampel DB, Dodson P, Osmólska H, 2nd ed., 259–322. University of California Press. https://doi.org/10.1525/california/9780520242098.003.0005.

Wagner GP, Altenberg L (1996). Perspective: complex adaptations and the evolution of evolvability. Evolution 50: 967–976.

Wagner GP, Pavlicev M, Cheverud JM (2007). The road to modularity. *Nature Review Genetics*, *8*: 921-931.

Walker AD (1990). A revision of *Sphenosuchus acutus* Haughton, a crocodylomorph reptile from the Elliot Formation (late Triassic or early Jurassic) of South Africa. Phil. Trans. R. Soc. Lond. B 220(1256): 1-120 http://doi.org/10.1098/rstb.1990.0185

Watanabe A, Slice DE (2014). The utility of cranial ontogeny for phylogenetic inference: A case study in crocodylians using geometric morphometrics. *Journal of Evolutionary Biology*, *27*(6): 1078–1092. https://doi.org/10.1111/jeb.12382

Welles SP (1984). *Dilophosaurus wetherilli* (Dinosauria, Theropoda): Osteology and Comparisons. *Palaeontographica. Abt. A. Bd.* 185: 85–180.

Werneburg I, Esteve-Altava B, Bruno J, Ladeira MT, Diogo R (2019). Unique Skull Network Complexity of Tyrannosaurus Rex among Land Vertebrates. *Scientific Reports* 9 (1): 1–14. https://doi.org/10.1038/s41598-018-37976-8.

Wilberg EW (2017). Investigating patterns of crocodyliform cranial disparity through the mesozoic and cenozoic. *Zoological Journal of the Linnean Society*, *181*(1), 189–208. https://doi.org/10.1093/zoolinnean/zlw027

Witmer LM (1997). The evolution of the antorbital cavity of archosaurs: A study in soft-tissue reconstruction in the fossil record with an analysis of the function of pneumaticity. *Journal of Vertebrate Paleontology* 17: 1–76. https://doi.org/10.1080/02724634.1997.10011027.

Worthy TH, Degrange FJ, Handley WD, Lee MSY (2017). The evolution of giant flightless birds and novel phylogenetic relationships for extinct fowl (Aves, Galloanseres). *R. Soc. open sci.*, 4. https://doi.org/10.1098/rsos.170975

Wu XC, Chaterjee S (1993). *Dibothrosuchus elaphros*, a crocodylomorph from the Lower Jurassic of China and the phylogeny of the Sphenosuchina. *Journal of Vertebrate Paleontology*, 13(1): 58-89. https://www.jstor.org/stable/4523486

You H, Dodson P (2004). "Basal Ceratopsia". In Weishampel DB, Dodson P, Osmolska H (eds.).

The Dinosauria (2nd ed.). Berkeley: University of California Press. 478–493.

Zhou CF, Gao KQ, Fox RC, Du XK (2007). Endocranial morphology of psittacosaurs (Dinosauria: Ceratopsia) based on CT scans of new fossils from the Lower Cretaceous, China. *Palaeoworld*. 16 (4): 285–293. doi:10.1016/j.palwor.2007.07.002

SUPPLEMENTARY MATERIALS

Table S1. Variance distribution across principal components

Table S2. First and last occurrence dates used to calibrate phylogenetic tree

Table S3. Internal nodes used for the phylogenetic tree

Table S4. Composition of modules for each taxon

Table S5. Categories of archosaurs based on capabilities of flight

Table S6. List of major fusion of bones with other bones in archosaurs

Table S7. Variation explained by each parameter

Table S8. Comparison of network-modules with modular hypotheses

Table S9. Distribution of bones based on modular hypotheses

Table S10. Topological network parameters measured for each taxon

Table S11. Network parameters categorized by diet

Table S12. Number of modules, Q value, and Q expected error generated.

Fig. S1. First two PC of topological parameters for all taxa.

Fig. S2. Second and third PC of topological parameters for all taxa.

Fig. S3. First and third PC of topological parameters for all taxa.

Fig. S4. First two PC of topological parameters for all taxa excluding avians.

Fig. S5. Second and third PC of topological parameters for all taxa excluding avians.

Fig. S6. First and third PC of topological parameters for all taxa excluding avians.

Fig. S7. First two PC of topological parameters for all taxa excluding adult avians.

Fig. S8. Second and third PC of topological parameters for all taxa excluding adult avians.

Fig. S9. First and third PC of topological parameters for all taxa excluding adult avians.

Fig. S10. Major events associated with changes in skull topological disparity for the first PC.

Supplementary Information 1 References and notes about the specimens used.

Supplementary Information 2 Comparison between network-modules and variational modules in archosaurs.

Supplementary Information 3 Comparison of network parameters among Aves, Crurotarsi, and non-avian Dinosauria.

Supplementary Information 4 Comparison based on diet.

Supplementary Information 5 Comparison of juvenile avian modules with adult avian bones.

Supplementary Information 6 Hypothesis Testing.

Supplementary Information 7 Supplementary Reference

FIGURE LEGENDS

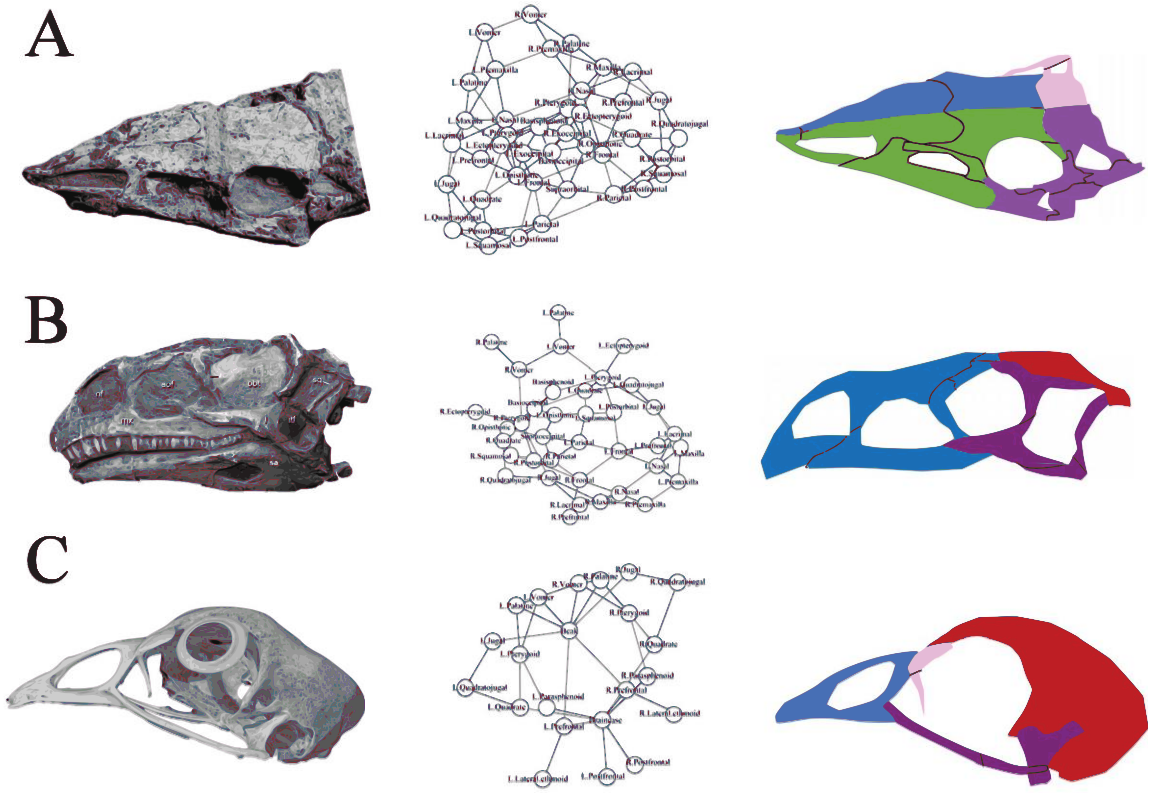

Figure 1. Anatomical network models. Example of the network models for three archosaurian skulls: (A) *Aetosaurus* from Schoch (2007); (B) *Plateosaurus* from Prieto-Marquez & Norell (2011); (C) *Gallus* from Digimorph. The pair-wise articulations among the bones of skulls (left) are formalized as network models (middle) and later analyzed, for example, to identify the skull anatomical modules (right). See methods for details.

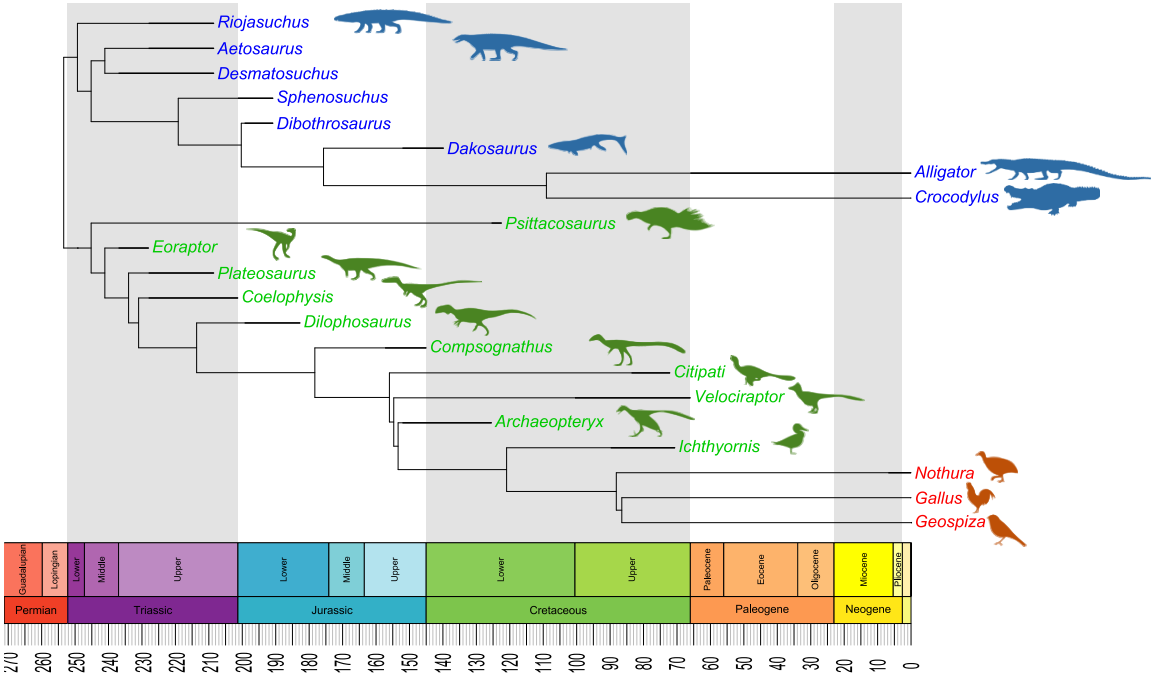

Figure 2. Phylogenetic framework. A phylogenetic tree was created based on the evolutionary relations among taxa as detailed in Galton & Upchurch (2004), Hailu & Dodson (2004), Holtz & Osmolska (2004), Norell & Makovicky (2004), Padian (2004), Tykoski & Rowe (2004), Upchurch et al (2004), Brusatte et al. (2010a), Nesbitt (2011), and Bhullar et al (2012). Bifurcation times were calibrated based on fossil dates from Benton and Donoghue (2007) using the equal method in the paleotree package. First and last occurrences were from Paleobiology Database. Silhouettes were from Phylopic.org. See methods for details.

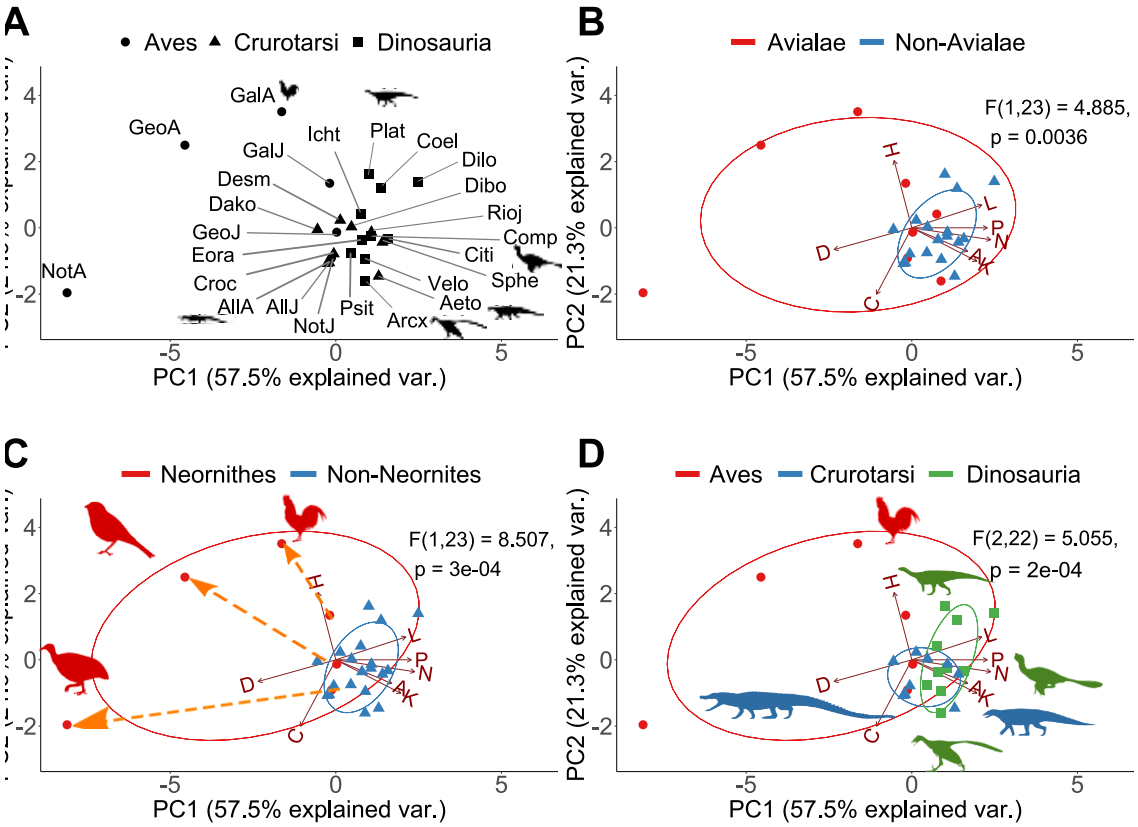

Figure 3. Principal components decomposition of topological variables. (A) Skull distribution for each taxon (see labels below). (B) Comparison of Aviale versus non-Aviale shows that non-Aviale occupy part of the Aviale morphospace. (C) Comparison of Neornithes versus non-Neornithes shows that non-Neornithes overlap with part of the Neornithes morphospace. Orange dotted arrows show the ontogenetic change in modern birds from juvenile stage to adult stage. (D) Comparison of Aves, Crurotarsi, and Dinosauria shows that they occupied different morphospace. Labels: N, Number of nodes; K, Number of links; D, Density of Connection; C, Mean clustering coefficient; H, Heterogeneity of connection; L, Mean path length; A, Assortativity of connection; P, Parcellation. Aeto, *Aetosaurus;* AllA, adult *Alligator*; AllJ, juvenile *Alligator*; Arcx, *Archaeopteryx*; Citi, *Citipati*; Coel, *Coelophysis*; Comp, *Compsognathus*; Croc, *Crocodylus*; Dako, *Dakosaurus*; Desm, *Desmatosuchus*; Dibo, *Dibothrosuchus*; Dilo, *Dilophosaurus*; Eora, *Eoraptor*; GalA, adult *Gallus*; GalJ, juvenile *Gallus*; GeoA, adult *Geospiza*; GeoJ, juvenile

Geospiza; Icht, *Ichthyornis*; NotA, adult *Nothura*; NotJ, juvenile *Nothura*; Plat, *Plateosaurus*; Psit, *Psittacosaurus*; Rioj, *Riojasuchus*; Sphe, *Sphenosuchus*; Velo, *Velociraptor*. Silhouettes were from Phylopic.org.

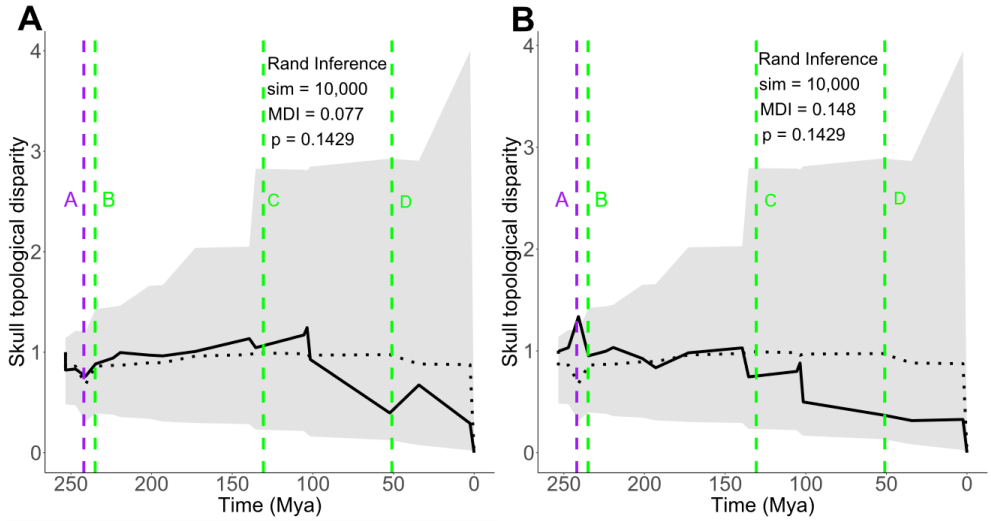

Figure 4. Topological disparity through time. Major events associated with major skull topological disparity for all taxa except juvenile extant taxa (A) and all taxa except adult taxa (B) using all phylogenetic PCAs with Brownian motion evolution from phytools package (Revell, 2012) and dtt function from geiger (Pennell et al. 2014). Skull topology disparity changed when the highest rates of morphological character evolution was recorded at 242 Mya (Event A, Naish & Barrett, 2016). A drop in topological disparity was observed around the period when modern bird lineages diversified (Event D, Brusatte et al. 2015; Jarvis et al. 2014) when adult modern birds were included (A) in the analysis. However, topological disparity evolution is not statistically significant difference from that expect in random simulations. Dotted black line showed the mean disparity from all random simulations; Grey areas marked the 95% confidence intervals of expected disparity based on 10,000 phylogenetic simulations (sim). MDI, the morphological disparity index, showed the difference between the relative observed disparity and the null hypothesis (Harmon et al. 2003). Colored vertical dashed lines mark key events,

including A: Highest rates of morphological character evolution 242 Mya (Naish & Barrett, 2016); B: Major increase in crurotarsan disparity and highest rates of morphological character evolution at 235 Mya (Naish & Barrett, 2016); C: Diversification of birds in Early Cretaceous from 130.7-120 Mya (Zhou et al. 2003; Zhou, 2014); D: Ordinal level of bird diversified 15mya after extinction and ended 50mya: 51-50 (Brusatte et al.2015; Jarvis et al. 2014).

5A

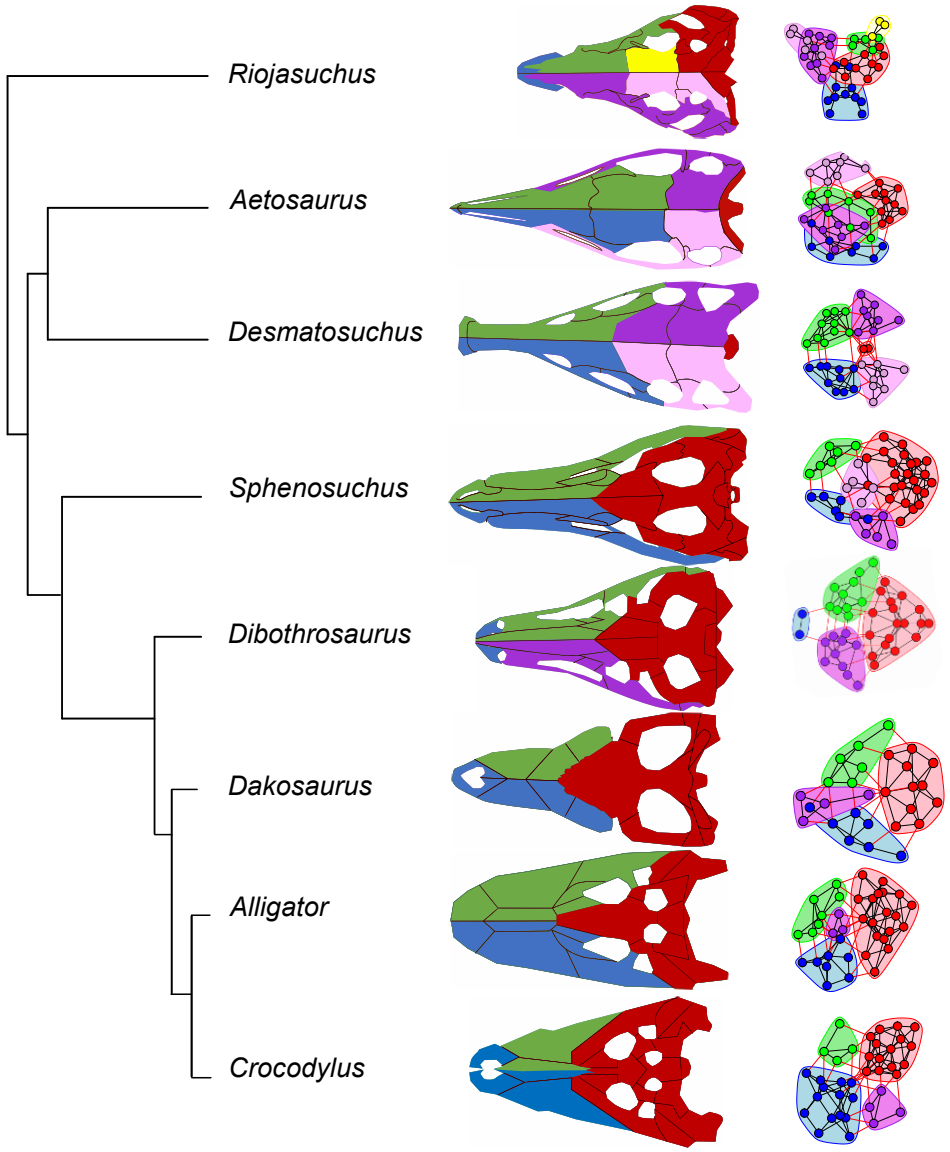
Riojasuchus
Aetosaurus
Desmatosuchus
Sphenosuchus
Dibothrosaurus
Dakosaurus
Alligator
Crocodylus

5B

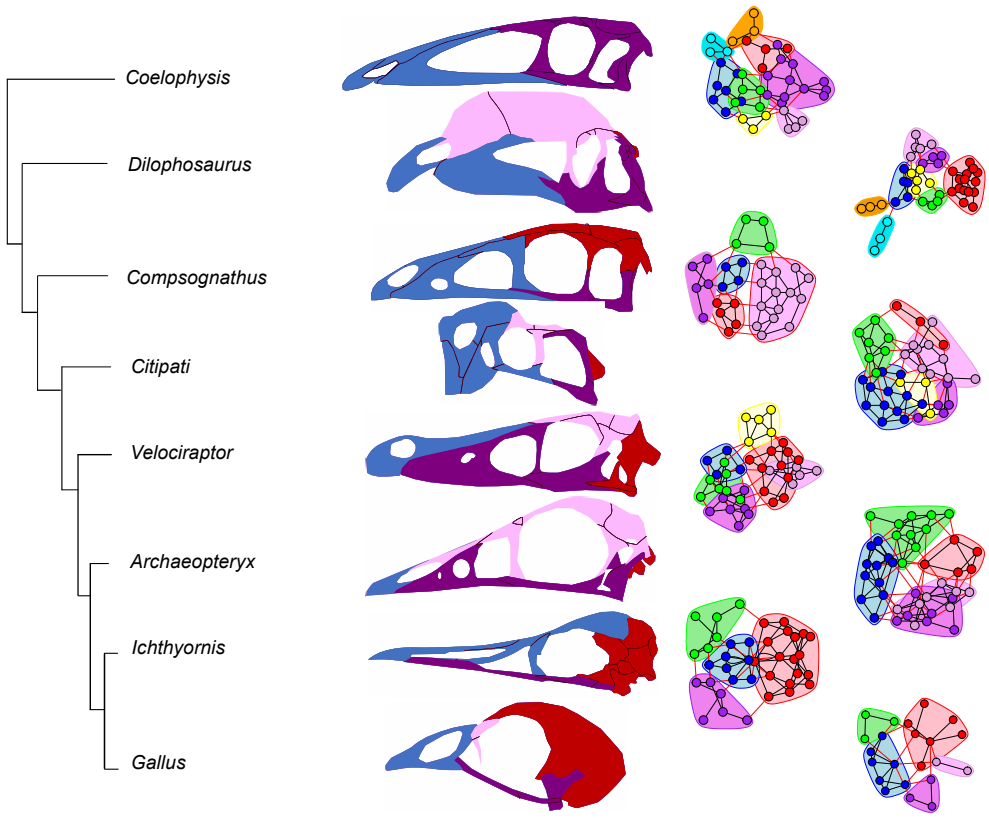
Coelophysis
Dilophosaurus
Compsognathus
Citipati
Velociraptor
Archaeopteryx
Ichthyornis
Gallus

5C

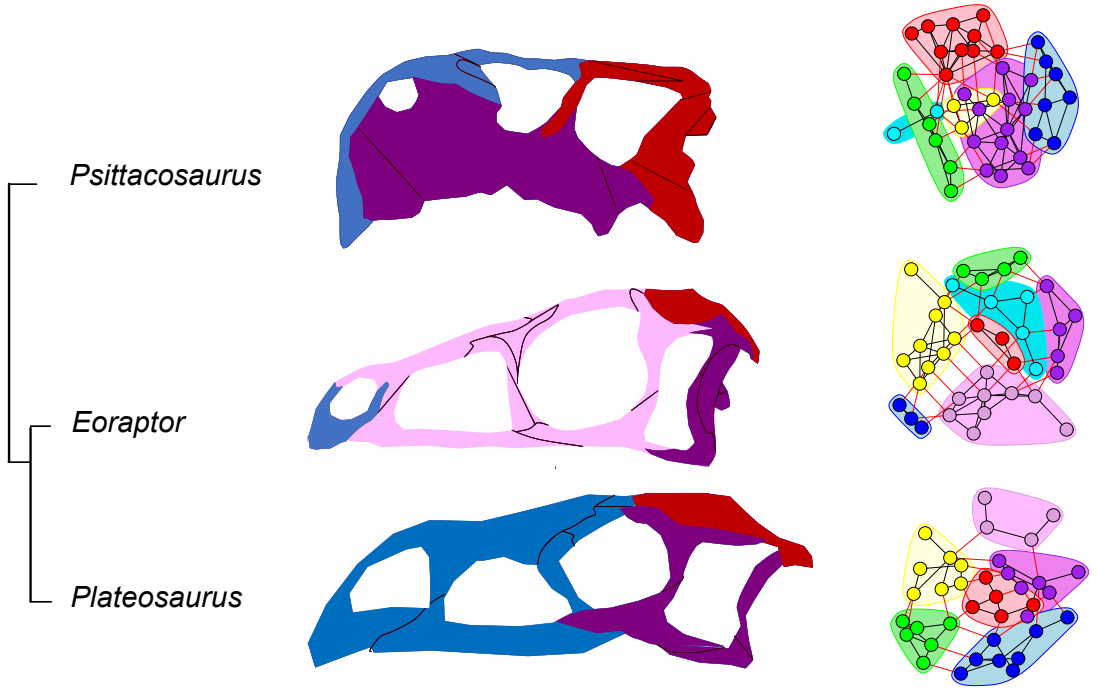

5D

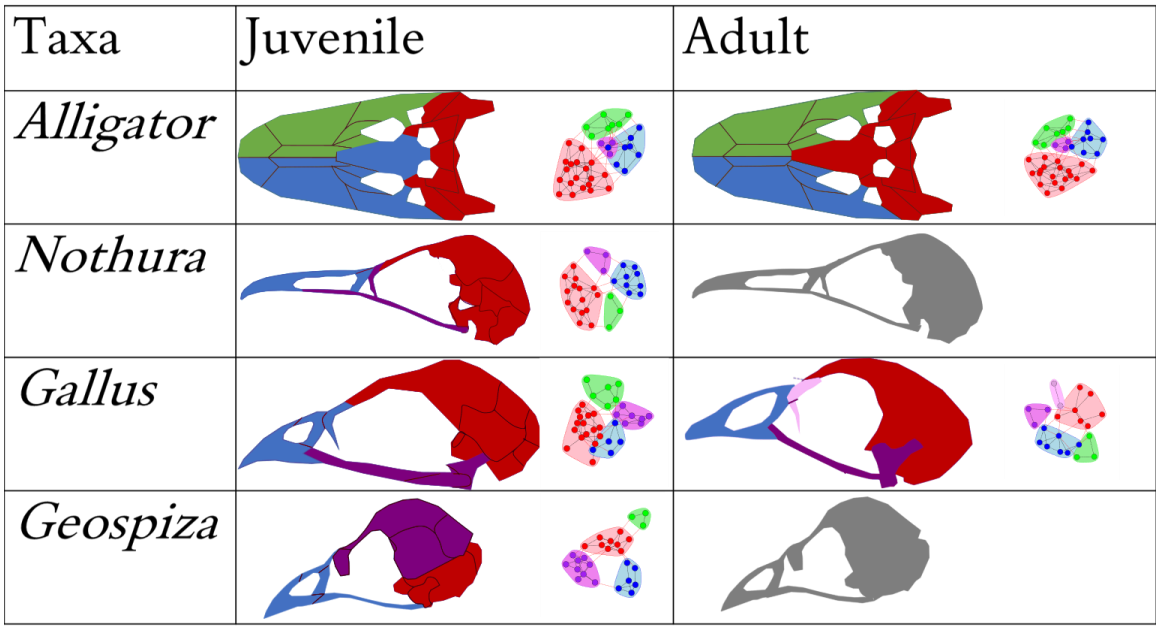

Figure 5. Visualizations of the module composition changes across phylogeny. The number of modules decreased from *Riojasuchus* (6) to *Crocodylus* (4, A) and from *Coelophysis* (8) to *Gallus* (5, B). The only exception is the transition from *Ichthyornis* (4) to adult *Gallus* (5). *Ichthyornis* have the same number of modules as juvenile *Gallus*, *Nothura* and *Geospiza* (D). (C) shows the difference in module composition among the ornithischian *Psittacosaurus*, the basal saurischian *Eoraptor*, and the auropodomorph *Plateosaurus*. (D) compares the adult and juvenile stages of extant species. Adult *Nothura* and *Geospiza* are shaded in grey as no modules were identified because of the small number of nodes and links due to a highly fused skull.

Left shows the modules as appeared on skulls, dorsal view for crurotarsans and left lateral view for Avemetatarsalia. Right shows the modules as appeared in networks. Composition of each module is listed in Supplementary Table 4.

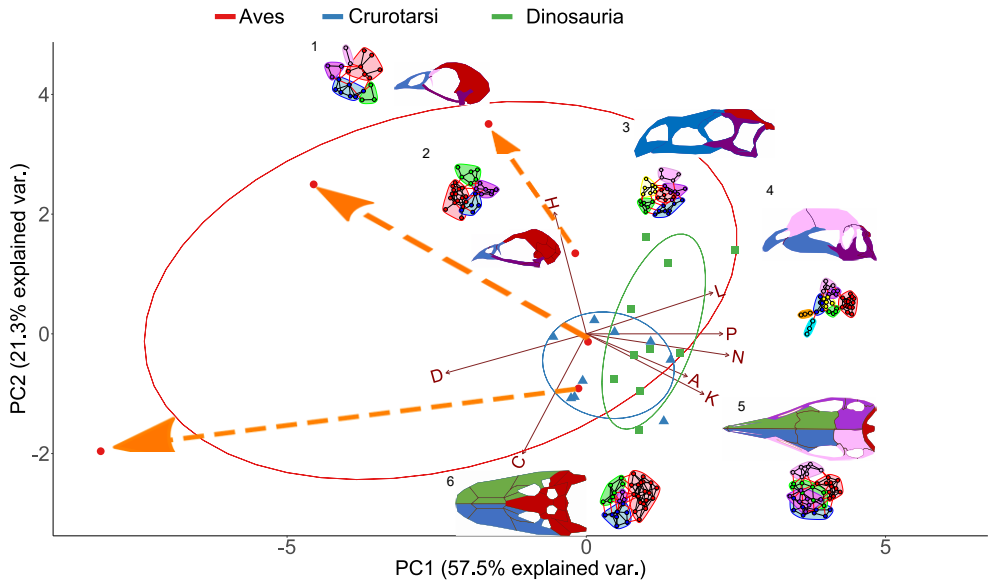

Figure 6. Overview of the evolution of archosaurs skull topology: Modern birds and some non-avian dinosaurs have more heterogeneous connections than crurotarsans; extant taxa have less bones and articulations than extinct ones; bones in juvenile modern birds fused and produce a more densely connected skull in the overall. Modules and networks of the following taxa are shown: (1) *Gallus*, (2) juvenile *Gallus*, (3) *Plateosaurus*, (4) *Dilophosaurus*, (5) *Aetosaurus*, (6) adult *Alligator*. Morphospace of Aves, Crurotarsi, and Dinosauria overlapped with each other. Orange arrows show the ontogenetic changes from juvenile to adult stages in neornithes. Taxa on the left side of the biplot have fewer modules and more bones, such as *Gallus* and *Alligator*, than taxa on the right, such as *Aetosaurus* and *Dilophosaurus*.